Supporting Information

Molecular Dynamics Simulations of PPI Dendrimer-Drug Complexes

Vaibhav Jain,[1] Vishal Maingi,[2] Prabal K. Maiti[2] and Prasad V. Bharatam[3]**

[1]*Department of Pharmacoinformatics, National Institute of Pharmaceutical Education and Research, Sector 67, S.A.S. Nagar, Punjab 160 062, India*

[2]*Centre for Condensed Matter Theory, Department of Physics, Indian Institute of Science, Bangalore 560 012, India*

[3]*Department of Medicinal Chemistry, National Institute of Pharmaceutical Education and Research, Sector 67, S.A.S. Nagar, Punjab 160 062, India*

S1. Methodology

S1.1. Building G5 PPI^{EDA} dendrimer using DBT

Dendrimer Builder Toolkit (DBT)[1] in conjunction with AMBER[2] was used to build initial geometry of G5 PPI^{EDA} (corresponding to low, neutral and high pH conditions) and G4 PPI^{DAB} (corresponding to neutral pH) dendrimers. For building G5 PPI^{EDA} dendrimer three residues were selected and named as ‘aaa’ (central core), ‘bbb’ (repeating fragment) and ‘ccc’ (terminal end). The structure of these residues is depicted in Figure S1. The branched Y shape structure of residue ‘bbb’ ensured that it will generate less entangled dendrimer geometry. In each of these residues a cap region was defined (shown in red (‘aaa’), blue (‘bbb’) and green (‘ccc’) regular circles in Figure S1). These caped regions were defined a constrained charge of zero and were removed before joining with the other residues. The atoms encircled in dashed rectangular boxes

represent the joining atoms. Capping atoms were selected in such a way that they mimic the atom types of joining atom and thus charge calculations would be accurate.

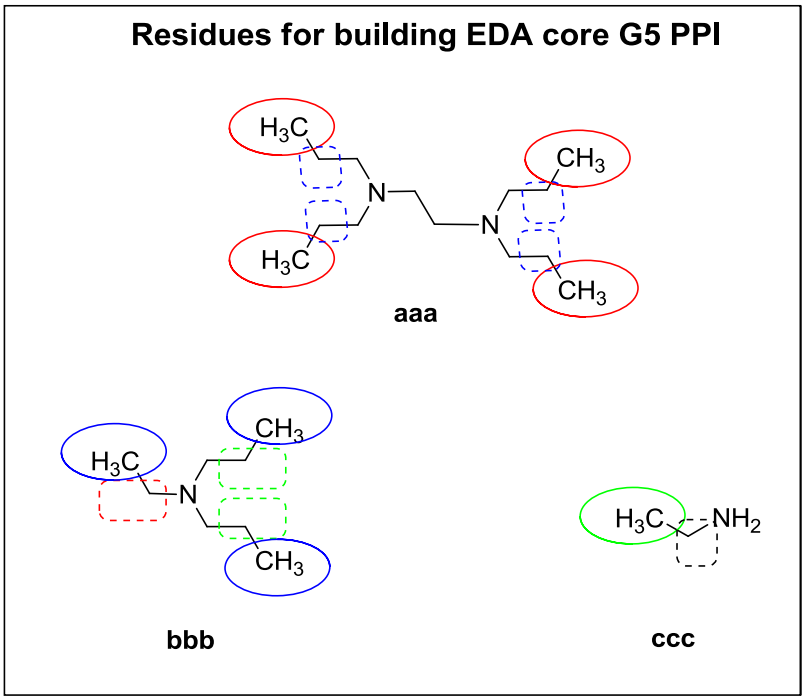

Figure S1. Residues selected for building G5 PPI^{EDA} dendrimer (Low pH- Full protonation, Neutral pH- 2/3 protonation, High pH- No protonation). Capping atoms defined in residues 'aaa', 'bbb' and 'ccc' are encircled red blue and green respectively. For GAFF atom types and partial atomic RESP charges please refer Table S1, S2 and S3.

All the residues (protonated and non-protonated) with caps were optimized individually using GAUSSIAN09[3] with HF/6-31G(d) as the basis set. During optimization, charges were calculated using ESP method. These optimized structures along with the ESP charges were given as input to the *antechamber* module of AMBER. In the *antechamber*, RESP charges were derived for the residues using two-stage RESP fitting method.[4] During the charge calculation the total charge of the cap atoms were constrained to zero, so that their removal will not affect the overall charge of the residue. For non-protonated residues (high pH), overall charge was set to

zero, while charge for protonated residues 'aaa' was kept +2 and for 'bbb' or 'ccc' +1 charge was assigned. *Antechamber* outputs were exported in *xleap* (another module of AMBER) as .mol2 files. The caps were then removed manually in *xleap* visualizer. De-capped residues so obtained were saved as *.lib* file (library file) and used further for building dendrimer using DBT. The 3D structure of protonated residues (after decapping) used for dendrimer building is shown in Figure S2. RESP partial atomic charges and GAFF atom types of residues are tabulated Tables S1, S2 and S3. The overall building process for building PPI^{EDA} dendrimer is represented in Figure S3. Similar methodology was adopted to build $G4^{DAB}$ PPI dendrimer (neutral pH) and residues used for the construction can be seen from our previous work.[1]

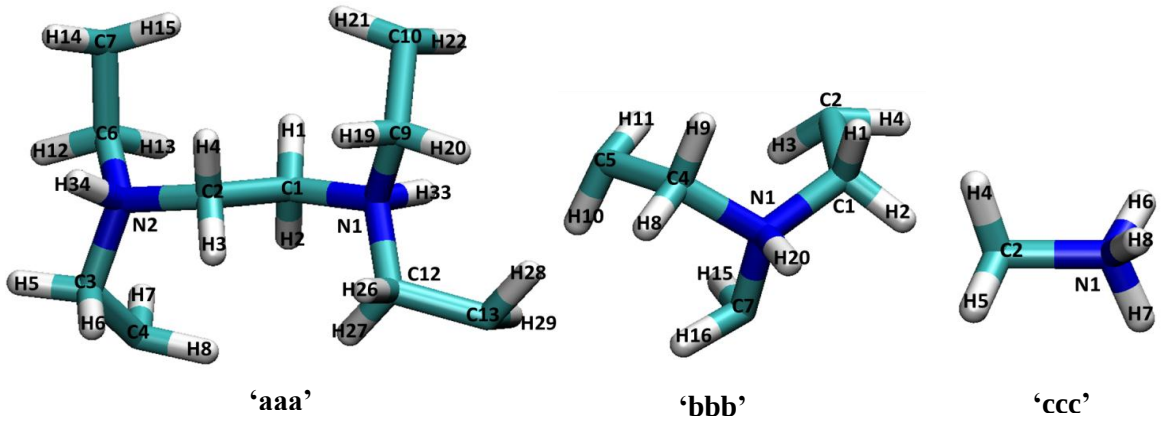

Figure S2. 3D structure of protonated residues at low pH 'aaa', 'bbb' and 'ccc' (after decapping) along with the atom numbers used for building G5 PPI^{EDA} (Low pH- Full protonation, Neutral pH- 2/3 protonation, High pH- No protonation). For GAFF atom types and RESP partial atomic charges please refer Tables S1, S2 and S3.

Table S1. GAFF atom types and RESP partial atomic charges of non-protonated and protonated 'aaa' residues used for building G5 PPI^{EDA} dendrimer.

Non-protonated			Protonated		
Atom	**GAFF atom type**	**Charge**	**Atom**	**GAFF atom type**	**Charge**
N1	n3	-0.471685	N1	n4	-0.080776
C1	c3	-0.051977	C1	c3	-0.014373
C2	c3	-0.051977	C2	c3	-0.014373
N2	n3	-0.471685	N2	n4	-0.080776
C3	c3	-0.039478	C3	c3	-0.023921
C4	c3	-0.033736	C4	c3	0.081217
H1	h1	0.103937	H1	hx	0.065680
H2	h1	0.103937	H2	hx	0.065680
C6	c3	-0.039478	C6	c3	-0.023921
C7	c3	-0.033736	C7	c3	0.081217
H3	h1	0.103937	H3	hx	0.065680
H4	h1	0.103937	H4	hx	0.065680
C9	c3	-0.039478	C9	c3	-0.023921
C10	c3	-0.033736	C10	c3	0.081217
H5	h1	0.074253	H5	hx	0.098534
H6	h1	0.074253	H6	hx	0.098534
C12	c3	-0.039478	C12	c3	-0.023921
C13	c3	-0.033736	C13	c3	0.081217
H7	hc	0.041301	H7	hc	0.042956
H8	hc	0.041301	H8	hc	0.042956
H12	h1	0.074253	H12	hx	0.098534
H13	h1	0.074253	H13	hx	0.098534
H14	hc	0.041301	H14	hc	0.042956
H15	hc	0.041301	H15	hc	0.042956
H19	h1	0.074253	H19	hx	0.098534
H20	h1	0.074253	H20	hx	0.098534
H21	hc	0.041301	H21	hc	0.042956
H22	hc	0.041301	H22	hc	0.042956
H26	h1	0.074253	H26	hx	0.098534
H27	h1	0.074253	H27	hx	0.098534
H28	hc	0.041301	H28	hc	0.042956
H29	hc	0.041301	H29	hc	0.042956
-	-	-	H33	hn	0.283237
-	-	-	H34	hn	0.283237
Sum (Σ)	-	0.000000	**Sum (Σ)**	-	2.000000

Table S2. GAFF atom types and RESP partial atomic charges of non-protonated and protonated 'bbb' residues used for building G5 PPI^{EDA} dendrimer.

Non-protonated			Protonated		
Atom	**GAFF atom type**	**Charge**	**Atom**	**GAFF atom type**	**Charge**
N1	n3	-0.429071	N1	n4	-0.060638
C1	c3	-0.043282	C1	c3	-0.090270
C2	c3	-0.034265	C2	c3	0.090620
H1	h1	0.068740	H1	hx	0.093185
H2	h1	0.068740	H2	hx	0.093185
C4	c3	-0.043282	C4	c3	-0.090270
C5	c3	-0.034265	C5	c3	0.090620
H3	hc	0.040880	H3	hc	0.034000
H4	hc	0.040880	H4	hc	0.034000
C7	c3	0.073811	C7	c3	0.158987
H8	h1	0.068740	H8	hx	0.093185
H9	h1	0.068740	H9	hx	0.093185
H10	hc	0.040880	H10	hc	0.034000
H11	hc	0.040880	H11	hc	0.034000
H15	h1	0.035937	H15	hx	0.058204
H16	h1	0.035937	H16	hx	0.058204
-	-	-	H20	hn	0.275803
Sum (Σ)	-	0.000000	**Sum (Σ)**	-	1.000000

Table S3. GAFF atom types and RESP partial atomic charges of non-protonated and protonated 'ccc' residues used for building G5 PPI^{EDA} dendrimer.

Non-protonated			Protonated		
Atom	**GAFF atom type**	**Charge**	**Atom**	**GAFF atom type**	**Charge**
C2	c3	0.181401	C2	c3	0.298107
H4	h1	0.040898	H4	hx	0.057331
H5	h1	0.040898	H5	hx	0.057331
N1	n3	-1.037731	N1	n4	-0.413974
H6	hn	0.387267	H6	hn	0.333735
H7	hn	0.387267	H7	hn	0.333735
-	-	-	H8	hn	0.333735
Sum (Σ)	-	0.000000	**Sum (Σ)**	-	1.000000

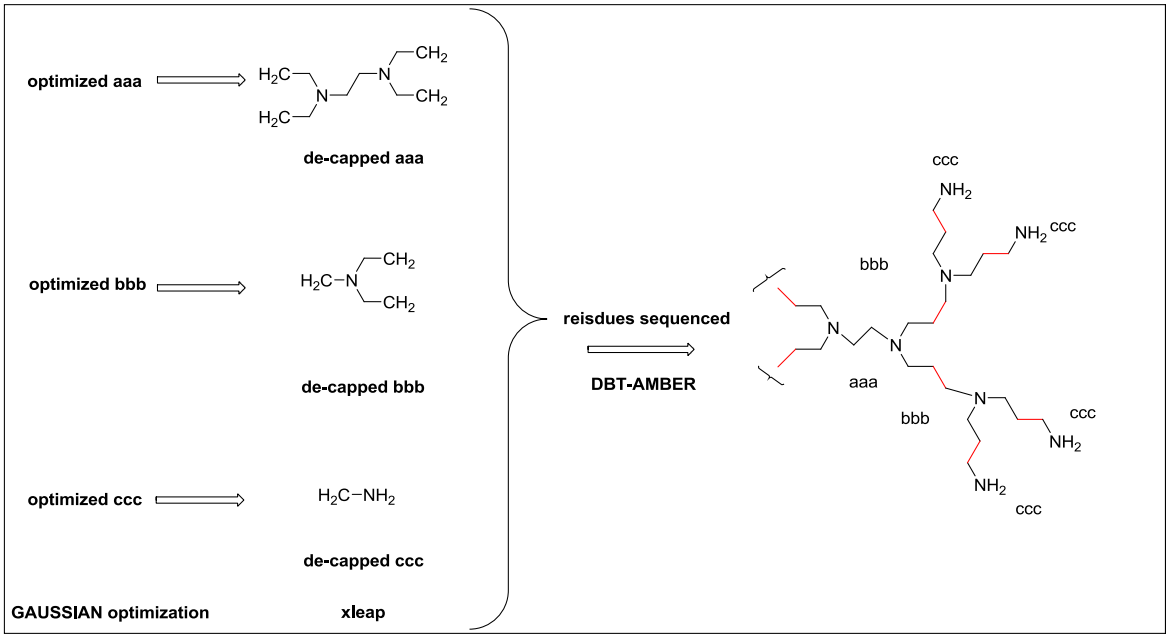

Figure S3. Simple logic for building G5 PPI^{EDA} dendrimer with DBT (see Figure S1 for 2D structure of 'aaa', 'bbb', and 'ccc'). Red bonds indicate the point of attachment for corresponding residues.

S1.2. Computational details for ligand processing

The 3D structure (see Figure 1, *Main manuscript*) of Famo (CSD Refcode: FOGVIG01), Indo (CSD Refcode: INDMET03) and Pbz (CSD Refcode: JAJKUB) drug molecules were retrieved from Cambridge Structural Database (CSD).[5] As per the pK_a of Famo (7.1), Indo (5.7) and Pbz (4.5), appropriate charged and uncharged species were considered while forming complexes with dendrimer for simulating at different pH conditions (see Table 2, *Main manuscript*).

In Famo, three protonation sites are possible (Figure S4) and each protonated species can exist in a wide variety of conformations. Thus, to determine the most plausible protonation site

of Famo, *ab initio* geometry optimization calculations were performed on possible sets of protonated drug species and their important conformers. *Ab initio* density functional theory (DFT)[6] calculations were performed using GAUSSIAN09 software package.[3] The gas phase geometry of all the species were fully optimized using B3LYP (Becke3, Lee, Yang, Parr) methods with 6-31+G(d,p) basis sets without any geometrical constraint. In order to understand the energetic behavior of these species in solvent (water), solvent level optimization studies were also performed using the integral equation formalism variant of the polarizable continuum model (IEFPCM) method[7] at 6-31+G(d,p) basis sets. Frequencies were computed analytically for all optimized species at all levels to characterize stationary points as minima or transition states and to estimate the zero point vibrational energies (ZPE). The calculated values (at 298.15K) have been scaled by a factor of 0.9806 for the B3LYP levels.

Electrostatic Potential (ESP) based partial atomic charges of all the drug molecules including their preferred protonated or deprotonated species were derived in GAUSSIAN09[3] with HF/6-31G(d) as the basis set. The output files obtained from the GAUSSIAN were used as an input for the *antechamber* to derive RESP partial atomic charges for the drug molecules. The GAFF atom types and RESP partial atomic charges of drug molecule Famo, Indo and Pbz are presented in Tables S4, S5 and S6 respectively.

Table S4. GAFF atom types and RESP partial atomic charges of neutral and protonated states of Famo drug molecule.

Neutral Famo			Protonated Famo		
Atom	**GAFF atom type**	**Charge**	**Atom**	**GAFF atom type**	**Charge**
N1	nh	-0.821007	N1	nh	-1.012668
N2	nh	-0.821007	N2	nh	-1.012668
C1	c2	0.717625	C1	cz	0.938289
N3	ne	-0.520556	N3	nh	-0.782571
C2	cc	0.385194	C2	cc	0.605009
N4	nd	-0.382988	N4	nd	-0.514127
C3	cd	0.030551	C3	cd	0.055710
C4	cc	-0.091366	C4	cc	-0.200750
S1	ss	-0.033102	S1	ss	-0.124857
C5	c3	-0.159243	C5	c3	-0.028482
S2	ss	-0.349365	S2	ss	-0.370689
C6	c3	0.506852	C6	c3	0.244122
C7	c3	-0.557144	C7	c3	-0.506069
C8	c2	0.579599	C8	c2	0.564326
N5	n2	-0.652408	N5	n2	-0.646810
S3	s6	1.254448	S3	s6	1.244861
O1	o	-0.604057	O1	o	-0.600671
O2	o	-0.604057	O2	o	-0.600671
N6	n3	-0.955108	N6	n3	-0.939690
N7	nh	-0.709279	N7	nh	-0.696957
H1	hn	0.446574	H1	hn	0.451033
H2	hn	0.446574	H2	hn	0.451033
H3	hn	0.446574	H3	hn	0.451033
H4	hn	0.446574	H4	hn	0.451033
H5	h4	0.264739	H5	h4	0.257505
H6	h1	0.168534	H6	h1	0.121865
H7	h1	0.168534	H7	h1	0.121865
H8	h1	-0.047065	H8	h1	0.042703
H9	h1	-0.047065	H9	h1	0.042703
H10	hc	0.215701	H10	hc	0.199697
H11	hc	0.215701	H11	hc	0.199697
H12	hn	0.450811	H12	hn	0.435196
H13	hn	0.450811	H13	hn	0.435196
H14	hn	0.368051	H14	hn	0.362402

H15	hn	0.368051	H15	hn	0.362402
-	-	-	H16	hn	-1.012668
Sum (Σ)	-	0.000000	**Sum (Σ)**	-	1.000000

Table S5. GAFF atom types and RESP partial atomic charges of neutral and anionic states of Indo drug molecule.

Neutral Indo			**Anionic Indo**		
Atom	**GAFF atom type**	**Charge**	**Atom**	**GAFF atom type**	**Charge**
Cl1	cl	-0.107488	Cl1	cl	-0.139567
O1	o	-0.560135	O1	o	-0.622944
O2	os	-0.371077	O2	os	-0.379052
O3	oh	-0.669312	O3	o	-0.913166
H1	ho	0.465045	O4	o	-0.913166
O4	o	-0.605114	N1	n	-0.227717
N1	n	-0.101243	C1	cc	0.020180
C1	cc	0.010003	C2	cd	0.054781
C2	cd	-0.160688	C3	ca	-0.051806
C3	ca	-0.027747	C4	ca	-0.048571
C4	ca	-0.163819	H1	ha	0.125437
H2	ha	0.160331	C5	ca	0.167337
C5	ca	0.200887	C6	ca	-0.272795
C6	ca	-0.213941	H2	ha	0.157965
H3	ha	0.163054	C7	ca	-0.178724
C7	ca	-0.215377	H3	ha	0.184909
H4	ha	0.199630	C8	ca	-0.018876
C8	ca	-0.001627	C9	c	0.904971
C9	c	0.732414	C10	ca	-0.247295
C10	ca	-0.151228	C11	ca	-0.111111
C11	ca	-0.142509	H4	ha	0.134442
H5	ha	0.153300	C12	ca	-0.056987
C12	ca	-0.055905	H5	ha	0.139311
H6	ha	0.144718	C13	ca	-0.008196
C13	ca	-0.008403	C14	ca	-0.056987
C14	ca	-0.055905	H6	ha	0.139311
H7	ha	0.144718	C15	ca	-0.111111
C15	ca	-0.142509	H7	ha	0.134442

H8	ha	0.153300	C16	c3	-0.395031
C16	c3	-0.185437	H8	hc	0.146314
H9	hc	0.095477	H9	hc	0.146314
H10	hc	0.095477	H10	hc	0.146314
H11	hc	0.095477	C17	c3	-0.077765
C17	c3	0.046148	H11	hc	-0.036256
H12	hc	0.035773	H12	hc	-0.036256
H13	hc	0.035773	C18	c	1.072579
C18	c	0.760639	C19	c3	0.024589
C19	c3	0.040267	H13	h1	0.068061
H14	h1	0.069011	H14	h1	0.068061
H15	h1	0.069011	H15	h1	0.068061
H16	h1	0.069011			-0.139567
Sum (Σ)	-	0.000000	**Sum (Σ)**	-	-1.000000

Table S6. GAFF atom types and RESP partial atomic charges of anionic Pbz drug molecule.

Anionic Pbz		
Atom	**GAFF atom type**	**Charge**
N1	n	-0.345193
C1	cc	0.724099
C2	cd	-0.553430
C3	c	0.724099
N2	n	-0.345193
C4	c3	-0.057613
C5	c3	0.046309
C6	c3	0.090290
C7	c3	-0.068746
O1	o	-0.675647
O2	o	-0.675647
C8	ca	0.229478
C9	ca	-0.090548
C10	ca	-0.242984
C11	ca	-0.145122
C12	ca	-0.242984
C13	ca	-0.090548
C14	ca	0.229478
C15	ca	-0.090548

C16	ca	-0.242984
C17	ca	-0.145122
C18	ca	-0.242984
C19	ca	-0.090548
H1	hc	0.031560
H2	hc	0.031560
H3	hc	0.004671
H4	hc	0.004671
H5	hc	-0.028104
H6	hc	-0.028104
H7	hc	-0.004878
H8	hc	-0.004878
H9	hc	-0.004878
H10	ha	0.119260
H11	ha	0.146367
H12	ha	0.118980
H13	ha	0.146367
H14	ha	0.119260
H15	ha	0.119260
H16	ha	0.146367
H17	ha	0.118980
H18	ha	0.146367
H19	ha	0.119260
Sum (Σ)	-	-1.000000

S1.3. Molecular docking

From the trajectories of MDs obtained for G5 PPI^{EDA} at different pH, representative equilibrated structure of dendrimers were extracted and used further for preparing corresponding drug-dendrimer complexes. In order to encapsulate drug inside the dendrimer, molecular docking approach was implemented using AUTODOCK 4.2 software.[8] Dendrimer and ligand molecules with RESP partial atomic charges were used in Autodock. Non polar hydrogens were not allowed to merge. For Indo and Pbz all the active torsions were allowed to rotate during docking, while in case of Famo, all the rotatable bonds except the bond between thiazole ring and

guanidine group were defined as active torsions for docking. This torsion angle was constrained in order to maintain the intramolecular hydrogen bonding between thiazole ring nitrogen and guanidine amino group.

The grid box was defined at the centre of macromolecule with 0.375 Å spacing and having 40 x 40 x 40 grid points in x, y and z direction respectively. The grid dimensions were large enough to cover the cavities around the central core ('aaa', Figure S2). Grid maps for dendrimer and drug molecule were generated with the help of auxiliary programme AutoGrid. Lamarckian genetic algorithm (GA)[9] was used for the purpose of docking. After implementing the above methodology a total of eight dendrimer–drug complexes (Table 3, *Main manuscript*) were obtained (G5 PPI^{EDA}-Famo and G5 PPI^{EDA}-Indo under three different pH conditions (low, neutral and high); G3 PAMAM-Pbz and G4 PPI^{DAB}-Pbz at neutral pH). The resulting molecular assemblies were taken up further for the simulation in AMBER.

S1.4. MM-PBSA Binding Free Energy Calculations

The molecular mechanical energies were calculated by *anal* program of AMBER 10. The Poisson Boltzmann solvation energies were calculated with the *pbsa* program of AMBER 10 using a grid spacing of 2 Å, dielectric constant for solute and solvent 1 and 80 respectively. For the calculation of nonpolar contributions, the solvent accessible surface area was calculated with *MSMS* program[10] of AMBER 10, by taking the solvent probe as 1.4 Å and the values for γ and β were set to 0.0072 kcal/mol/$Å^2$ and 0.0 kcal/mol respectively.

S2. Results and Discussion

S2.1. Quantum chemical analysis of Famotidine (Famo)

At different pH, Famo drug molecule (pK_a = 7.1) can either exist in neutral or protonated form (pH 4 - protonated, pH 7.4 & 10 - neutral). Three protonation sites are possible in Famo as shown in Figure S4. The crystal structure of neutral (CSD Refcode: FOGVIG01) as well as protonated form (CSD Refcode: JATLOF, Famotidine hydrochloride) of Famo is available in CSD. In the protonated form, protonation is reported at the guanidine nitrogen atom attached to thiazole ring. Moreover in the crystal structures, an intramolecular hydrogen bonding between the guanidine amino group and ring nitrogen of thiazole moiety has also been observed.

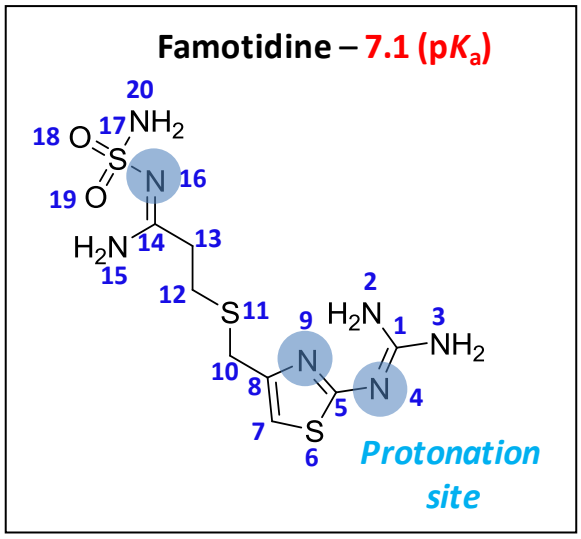

Figure S4. 2D structure of Famotidine (Famo) along with atom numbering and possible sites of protonation.

In order to identify most preferred protonation site of Famo, three different protonated species were considered along with their important conformers. All of them were optimized at

B3LYP/6-31+G(d,p) level in gaseous as well as in solvent phase (water, IEFPCM method) conditions using GAUUAIN09 software. After full optimization, they were named as **Famo-H1** (protonation at N4), **Famo-H2** (protonation at N9) and **Famo-H3** (protonation at N14), while their corresponding rotamers (obtained after rotating C1-N4-C5-N9 torsion angle to 180^{o}) were designated as **Famo-H1rot**, **Famo-H2rot** and **Famo-H3rot**. The 3D structure of these protonated species after optimization in solvent phase are depicted in Figure S5 and the relative energies of these species in gaseous as well as solvent phase are presented in Table S7. In all the structures intramolecular hydrogen bonding N15-H•••O19 was observed, while in all the rotamers weak intramolecular interaction N2-H•••S6 was also seen in addition.

In gas phase, the most stable structure **Famo-H2rot** is stabilized by the intramolecular hydrogen bonding C7-H•••O18 in addition to above mentioned interactions. **Famo-H3rot** was found to be energetically the least favourable structure by about 21.61 kcal/mol on a relative energy scale. Likewise, **Famo-H3** and **Famo-H1rot** were less stable by ~14 kcal/mol. In case of **Famo-H3** and **Famo-H3rot**, the extended conformation of sulfamoylpropanamidine side chain was observed (as compared to bent conformations in all other structures) due to which hydrogen bonding C7-H•••O18 gets broken. Thus the possibilities of these two structures are ruled out. In case of **Famo-H2**, due to the protonation at ring nitrogen of thiazole moiety (N9), hydrogen-hydrogen repulsion and twisting of guanidine side chain occurs that leads to abolish the intramolecular hydrogen bonding with guanidine N2H. But still **Famo-H2** is more stable than **Famo-H1** by about 2.08 kcal/mol which showed strong intramolecular hydrogen bonding N2-H•••N. In order to obtain more accurate results mimicking experimental conditions, solvent phase optimization calculations in water were performed on all the protonated structures. After full optimization in solvent phase, **Famo-H1** and **Famo-H2rot** becomes almost isoenergetic,

whereas **Famo-H3rot** was again turned out to be the least stable structure (~ 15.74 kcal/mol). In agreement with X-ray diffraction and 1H NMR studies,[11] the most stable structure **Famo-H1** maintains the strong hydrogen bond anchoring the guanidine chain in the same plane as the thiazole ring. Due to this co-planarity, conjugation of guanidine with the thizaole ring was observed, while in all the rotamers the communication of atomic arrangement is missing as they all are out of plane. Since, implicit solvent phase optimization studies reflects the more realistic picture, thus the result obtained herewith was considered for assigning the most plausible protonation site of Famo. Finally, **Famo-H1** was considered as the correct representation of the protonated species and used further for the complexation with dendrimer and simulation at low pH. The results obtained in this study are in concurrence with the semi-empirical calculations performed by Olea-Azar and Parra-Mouchet[12] on Famo and its analogues. Moreover, recently reported NMR-pH titration study on Famo drug molecule also corroborate our observation.[13]

Table S7. Relative energies (kcal/mol) of possible protonated species of Famo drug molecule after optimization in gaseous as well as in solvent phase at B3LYP-6-31+G(d) level.

Name	**Relative energies (kcal/mol) B3LYP/6-31+G(d,p)**	
	Gas phase	**Solvent phase (water, IEFPCM)**
Famo-H1	6.16	0.00
Famo-H2	4.08	2.38
Famo-H3	14.56	10.29
Famo-H1rot	14.32	5.43
Famo-H2rot	0.00	0.05
Famo-H3rot	21.61	15.74

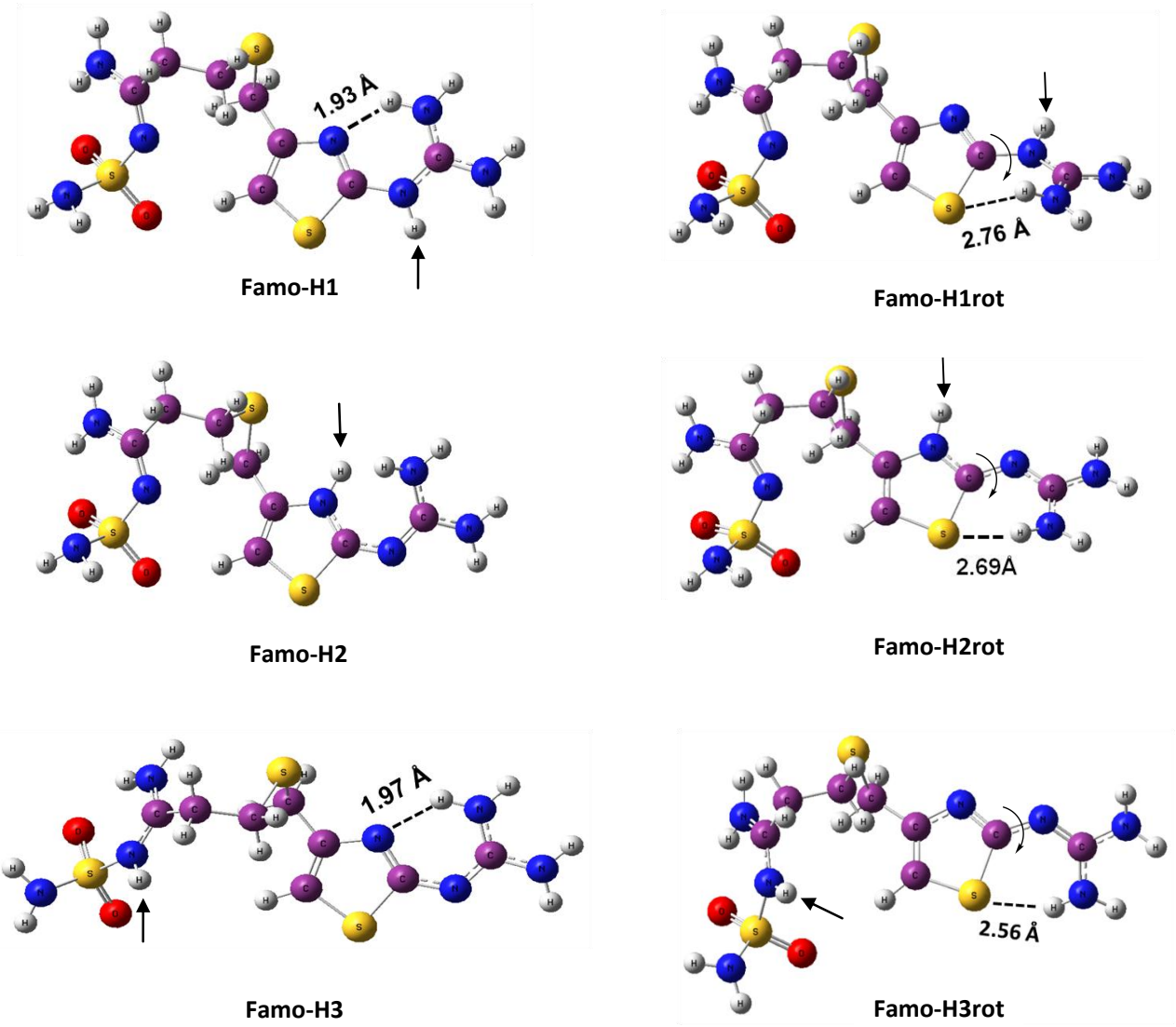

Figure S5. B3LYP-6-31+G(d) optimized geometries (solvent phase) of various protonated species of Famo drug molecule. Black arrow indicates the site of protonation considered.

S2.2. Hydrogen bond analysis between peripheral amines (ccc residue) and water

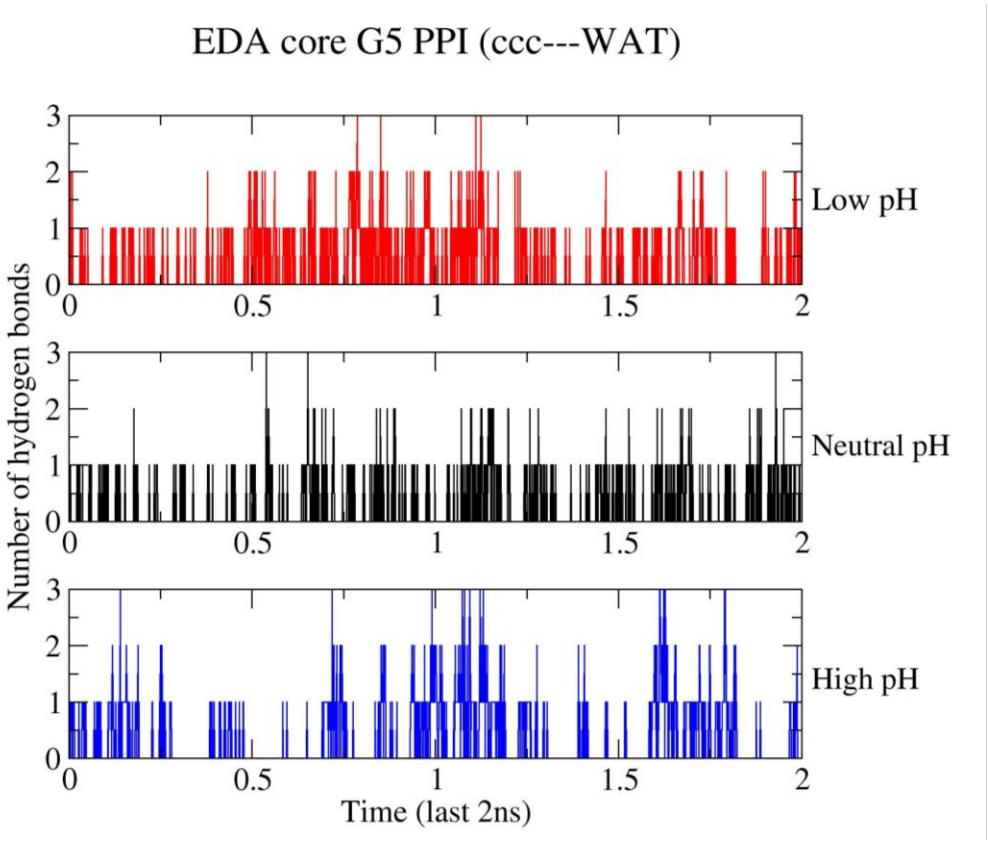

Figure S6. Number of hydrogen bonds formed between terminal primary amines (ccc) of G5 PPI^{EDA} and water molecules at low, neutral and high pH conditions (analysis was performed on the last 2 ns or 2000 snapshots of the total simulation run). For calculating hydrogen bonds, angle and distance cutoff was set to 120^{o} and 3.0 Å respectively.

2.3. Molecular Dynamics Simulation Analysis of Dendrimer-Drug Complexes

(a) G5 PPI^{EDA}-Famo (Low pH)

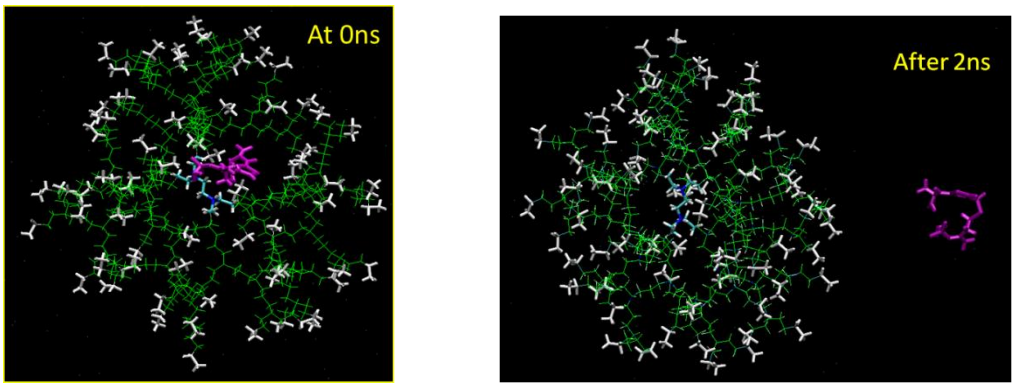

(b) G5 PPI^{EDA}-Famo (Neutral pH)

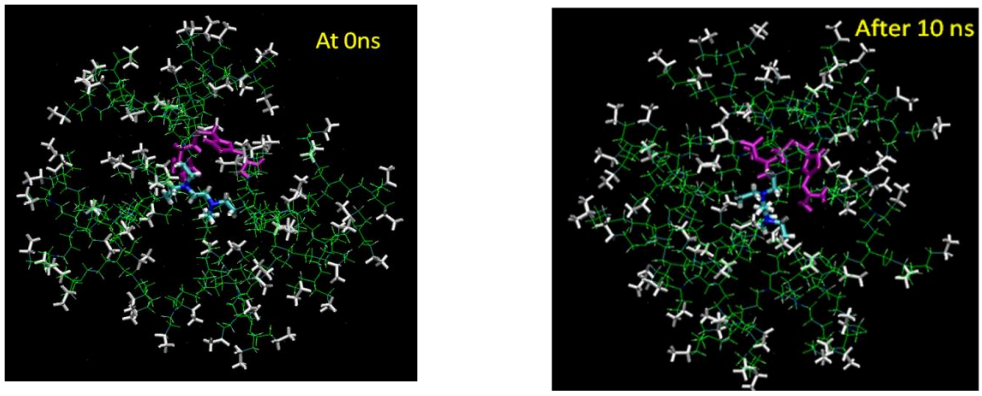

(c) G5 PPI^{EDA}-Famo (High pH)

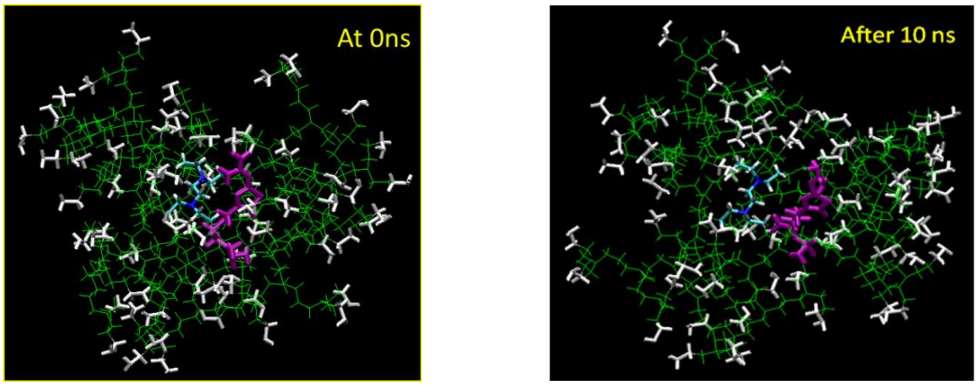

Figure S7. Snapshots of G5 PPI^{EDA}-Famo complex during different time intervals of MD simulation run at various pH conditions **(a)** low pH **(b)** neutral pH and **(c)** high pH. Colour coding and molecule/fragment representation is as follows: *Magenta sticks* – Famo; *Blue and cyan sticks* – core ('aaa' residue); Green lines – repeating fragments ('bbb' residue); *White sticks* –terminal amino groups ('ccc' residue).

(a) G5 PPI^{EDA}-Indo (Low pH)

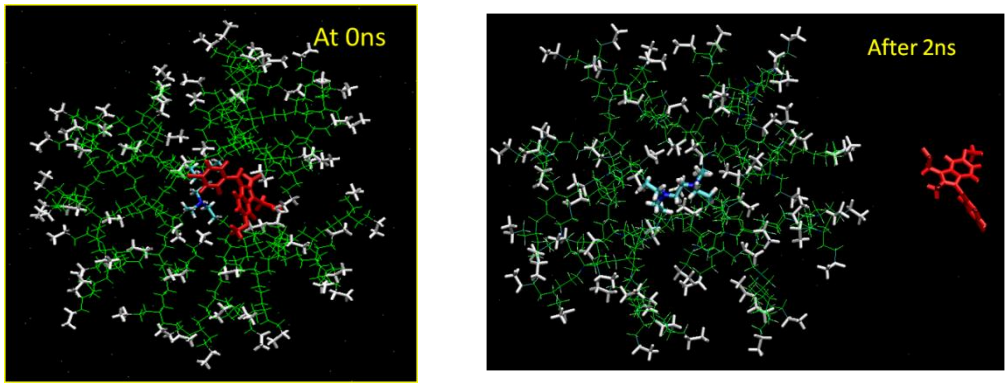

(b) G5 PPI^{EDA}-Indo (Neutral pH)

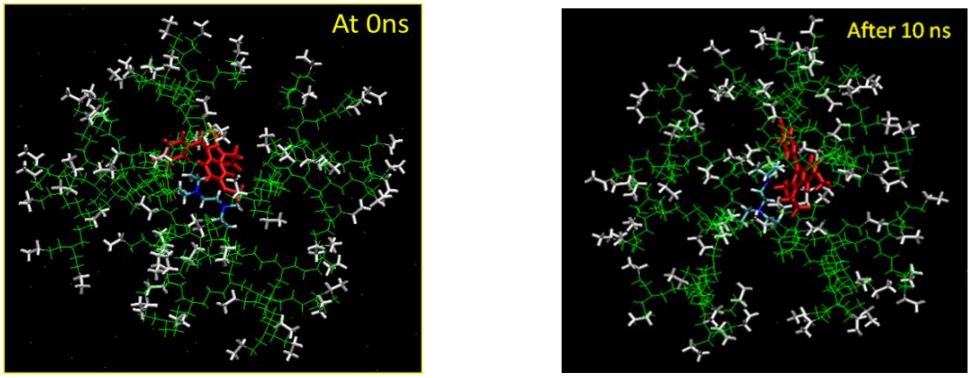

(c) G5 PPI^{EDA}-Indo (High pH)

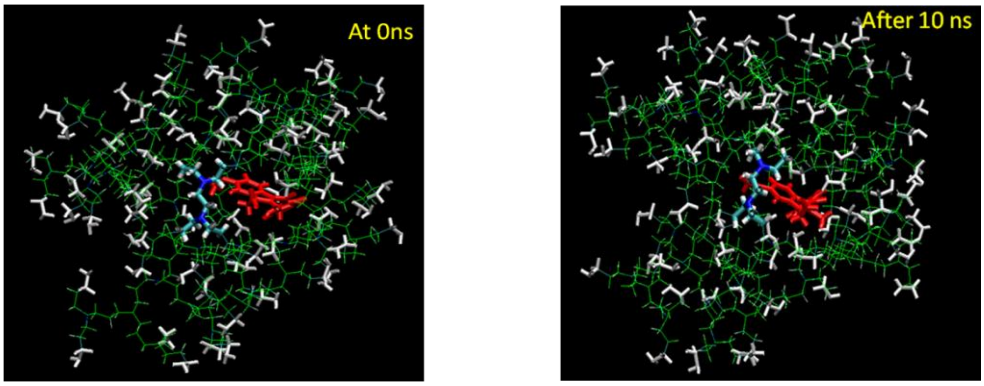

Figure S8. Snapshots of G5 PPI^{EDA}-Indo complex during different time intervals of MD simulation run at various pH conditions **(a)** low pH **(b)** neutral pH and **(c)** high pH. Colour coding and molecule/fragment representation is as follows: *Red sticks* – Indo; *Blue and cyan sticks* – core ('aaa' residue); Green lines – repeating fragments ('bbb' residue); *White sticks* – terminal amino groups ('ccc' residue).

2.4. MM-PBSA Binding Free Energy Analysis

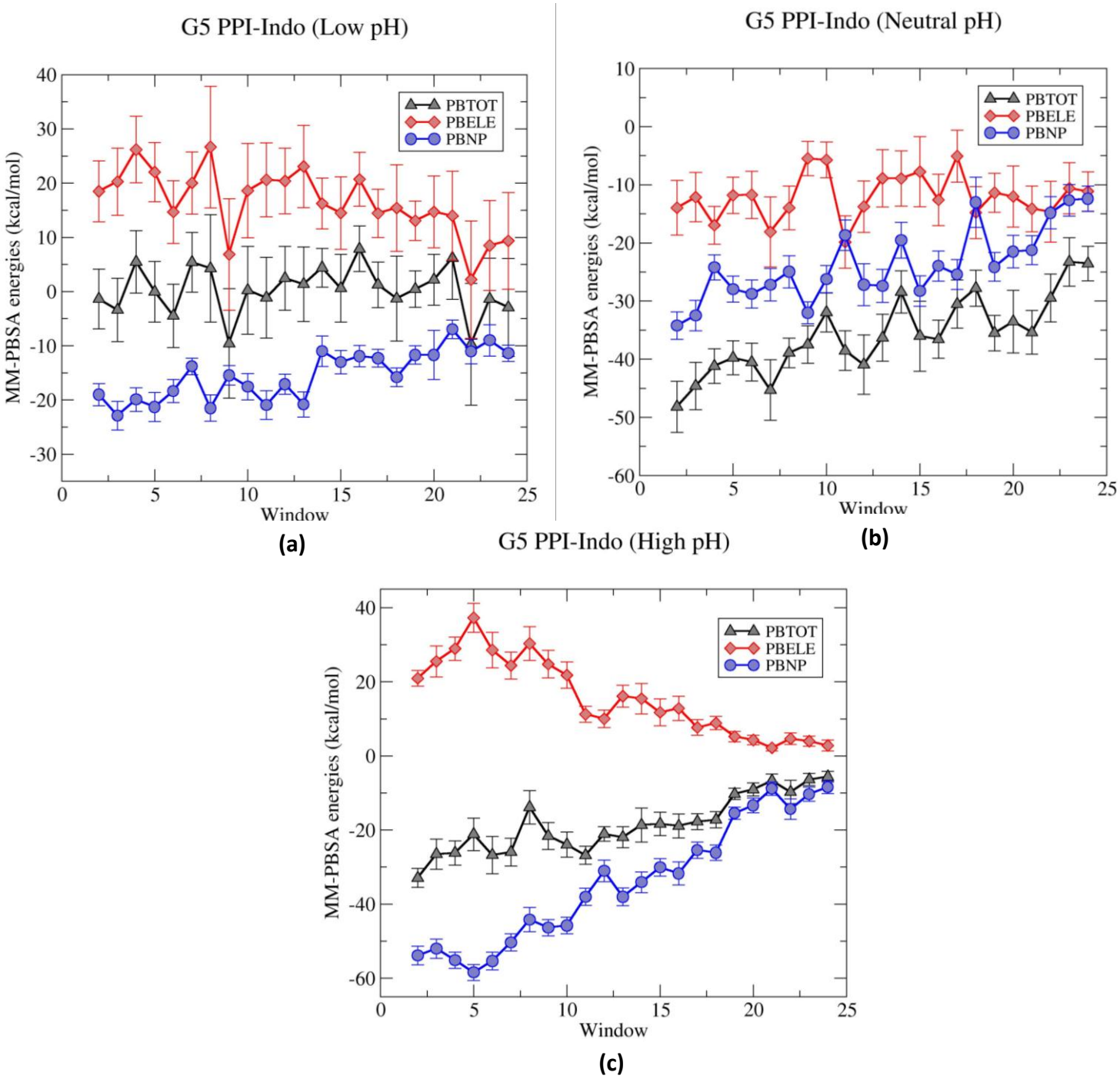

Figure S9. Plots (with Std. Dev. bars) showing different energy components of MM-PBSA for G5 PPI^{EDA}-Indo complex at **(a)** low pH, **(b)** neutral pH and **(c)** high pH. **PBTOT** = **PBELE** + **PBNP**. *Abbreviations:* PBTOT = Final estimated binding free energy, PBELE = Electrostatic solvation free energy (PBCAL) + MM electrostatic energy (ELE), PBNP = nonpolar solvation free energy (PBSUR) + MM van der Waals energy (VDW).

S2.5. Hydrogen bond analysis between drug Indo and G5 PPI^{EDA} dendrimer

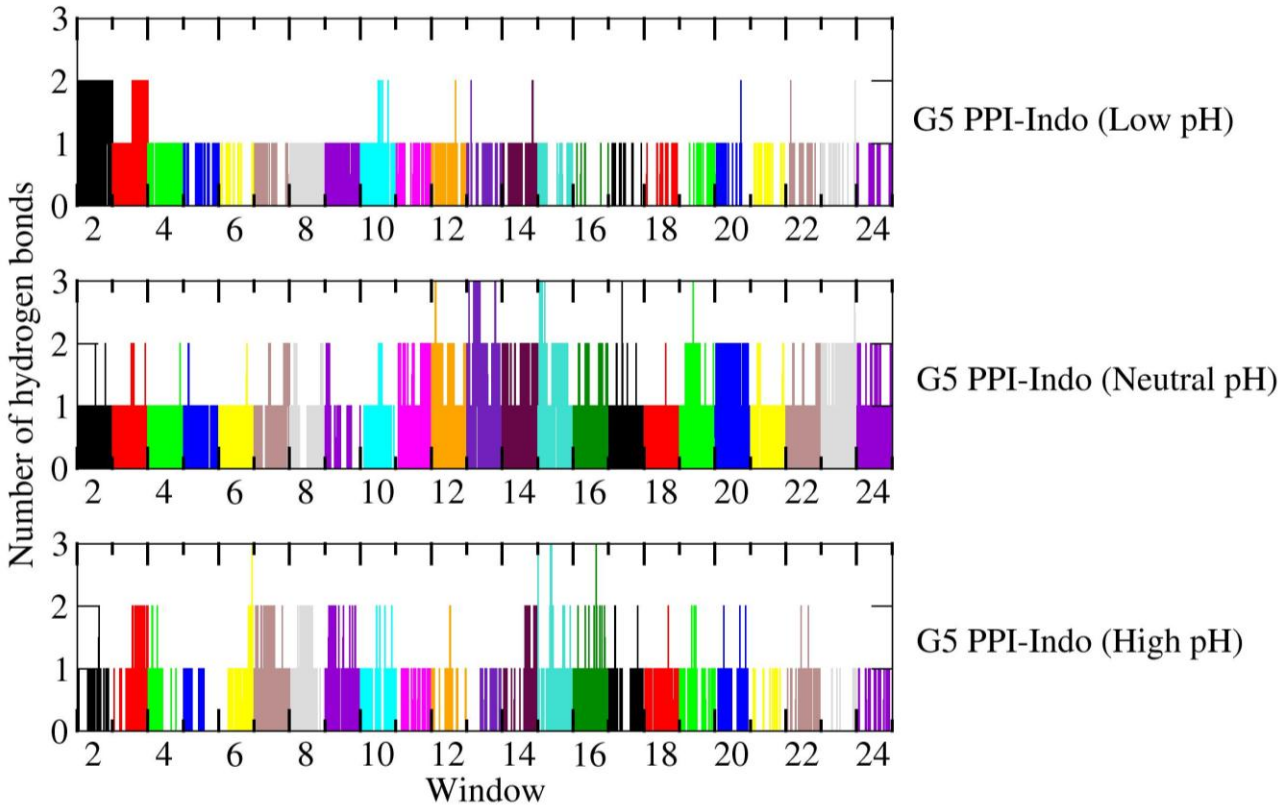

Figure S10. Plots showing hydrogen bonds formation ability of drug molecule Indo (carboxylic, methoxy and carbonyl groups) with the G5 PPI^{EDA} dendrimer (primary and tertiary amino groups) at low, neutral and high pH conditions. X axis represents the umbrella sampling window (each 1ns simulation run and hydrogen bonds were calculated on each snapshot after 1ps). For calculating hydrogen bonds, angle and distance cutoff was set to 120^{o} and 3.0 Å respectively.

.

S2.6. Radius of gyration for drug loaded dendrimers

To identify the conformational changes in dendrimer after drug loading, Radius of gyration (R_g) of the G5 PPI^{EDA} dendrimer (with Famo and Indo) at all the three pH conditions (Figure S11a) as well as G3 PAMAM and G4 PPI^{DAB} dendrimers (with Pbz) (Figure S11b) at neutral pH conditions were analyzed for all the umbrella sampling windows.

In case of Famo and Indo loaded G5 PPI^{EDA} dendrimer at low and neutral pH conditions (Figure S11a), R_g values were found to be consistent and almost close to the R_g values of the drug unloaded equilibrated dendrimer (Low pH – 16.29 Å, Neutral pH – 15.77 Å). This is because, protonation of primary and tertiary amines causes electrostatic repulsions which resulted in swelling of the dendrimer, and in such "open" structures the size of inner cavities are large enough to host the drug molecules easily. In contrary, at high pH where the structure is quite compact the R_g values of drug loaded G5 PPI^{EDA} dendrimer deviates to some extent from the R_g values of the drug unloaded equilibrated dendrimer (High pH – 12.73 Å). In detail, two different trends of deviation were observed at high pH, in case of Famo loaded G5 PPI^{EDA} dendrimer R_g values slightly decreases, while in case of Indo loaded G5 PPI^{EDA} dendrimer R_g values slightly increases (Figure S11a). The reason being, Famo is more flexible as compared to Indo (in terms of number of rotatable bonds), thus Famo can adopt various conformation which can be easily encapsulated in the compact structure of dendrimer. Another reason could also be attributed to intermolecular hydrogen bonding i.e. in an attempt to maximize the hydrogen bonding between Famo and atoms of the dendrimer the overall R_g slightly decreases. Intermolecular hydrogen bonding analysis of G5 PPI^{EDA}-Famo complex (Figure 8, *main manuscript*) also showed that these interactions are more at high pH. On the other hand, when Indo is pushed inside the G5

PPI^{EDA} dendrimer because of the bigger size and higher rigidity of Indo in comparison to Famo, slight increase in overall R_g of the dendrimer was observed. Accordingly, Indo faces larger free energy barrier as compared to Famo in G5 PPI^{EDA} dendrimer at high pH conditions.

In case of G3 PAMAM-Pbz and G4 PPI^{DAB}-Pbz complexes at neutral pH, no significant change in the R_g was observed for the dendrimers when compared with the R_g value of drug unloaded equilibrated dendrimers (G3 PAMAM – 15.78 Å, G4 PPI^{DAB} – 12.97 Å). Here also, the same swelling concept and large size of the internal cavities at neutral pH are responsible for the easy encapsulation of Pbz in G3 PAMAM and G4 PPI^{DAB}, without much change in the dendrimers conformation.

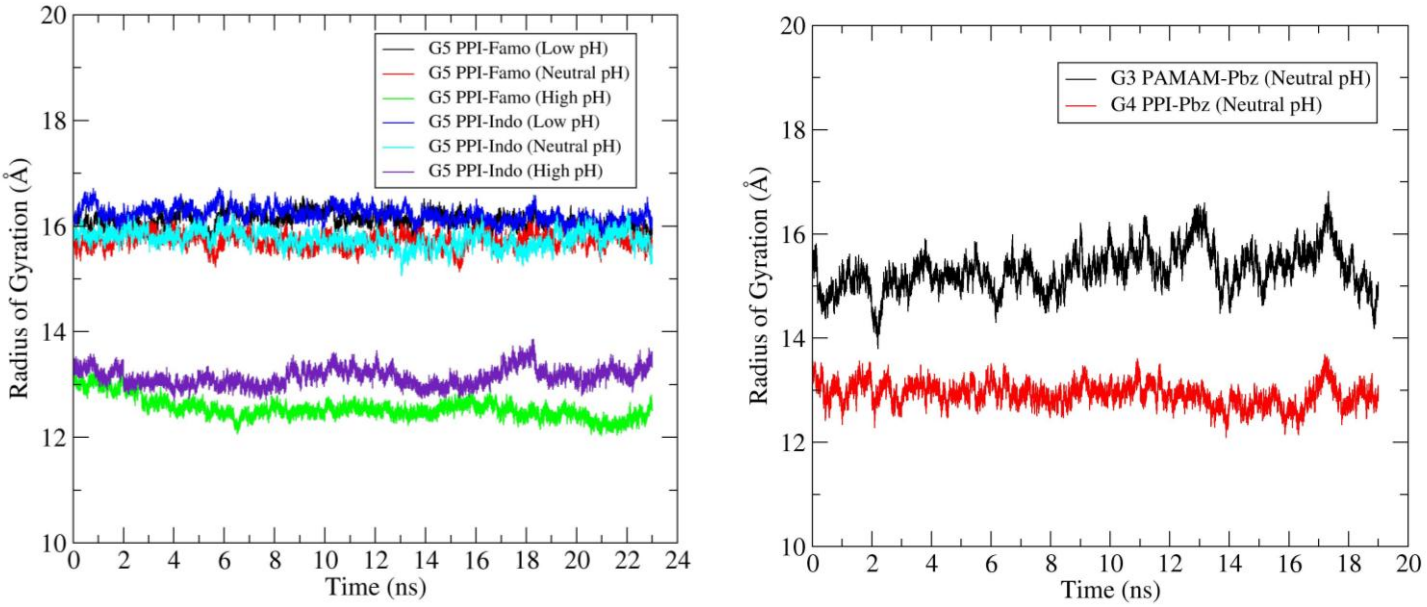

Figure S11. Time evolution of Radius of Gyration (R_g) of the drug loaded dendrimer for the complete umbrella sampling windows (each snapshot being saved at 1 ps). **(a)** G5 PPI^{EDA}-Famo and G5 PPI^{EDA}-Indo complexes at low, neutral and high pH conditions. **(b)** G3 PAMAM-Pbz and G4 PPI^{DAB}-Pbz complexes at neutral pH condition.

References

1. V. Maingi, V. Jain, P. V. Bharatam and P. K. Maiti, *J. Comput. Chem.*, 2012, **33**, 1997–2011. http://www.physics.iisc.ernet.in/~maiti/dbt/home.html.

2. D. A. Case, T. A. Darden, T. E. Cheatham III, C. L. Simmerling, J. Wang, R. E. Duke, R. Luo, M. Crowley, R. C. Walker, W. Zhang, K. M. Merz, B. Wang, S. Hayik, A. Roitberg, G. Seabra, I. Kolossváry, K. F. Wong, F. Paesani, X. Wu, S. Brozell, T. Steinbrecher, H. Gohlke, L. Yang, C. Tan, J. Mongan, V. Hornack, G. Cui, D. H. Mathews, M. G. Seetin, C. Sagui, V. Babin and P. A. Kollman, University of California, San Francisco, 2008.

3. M. Frisch, G. Trucks, H. Schlegel, G. Scuseria, M. Robb, J. Cheeseman, G. Scalmani, V. Barone, B. Mennucci, G. Petersson and H. Nakatsuji, Gaussian, Inc., Wallingford CT, 2010.

4. C. I. Bayly, P. Cieplak, W. Cornell and P. A. Kollman, *J. Phys. Chem.*, 1993, **97**, 10269-10280.

5. F. H. Allen, *Acta Crystallogr. Sect. B: Struct. Sci.*, 2002, **58**, 380-388.

6. R. G. Parr and W. Yang, *Density-functional theory of atoms and molecules*, Oxford University Press, USA, 1994.

7. M. Cossi, G. Scalmani, N. Rega and V. Barone, *J. Chem. Phys.*, 2002, **117**, 43-54.

8. D. S. Goodsell, G. M. Morris and A. J. Olson, *J. Mol. Recognit.*, 1996, **9**, 1-5.

9. G. M. Morris, D. S. Goodsell, R. S. Halliday, R. Huey, W. E. Hart, R. K. Belew and A. J. Olson, *J. Comput. Chem.*, 1998, **19**, 1639-1662.

10. M. F. Sanner, A. J. Olson and J. C. Spehner, *Biopolymers*, 1996, **38**, 305-320.

11. T. Ishida, Y. In, M. Shibata, M. Doi, M. Inoue and I. Yanagisawa, *Mol. Pharmacol.*, 1987, **31**, 410-416.

12. C. Olea-Azar and J. Parra-Mouchet, *J. Mol. Struc.-THEOCHEM*, 1997, **390**, 239-245.

13. A. Marosi, Z. Szalay, S. Beni, Z. Szakacs, T. Gati, A. Racz, B. Noszal and A. Demeter, *Anal. Bioanal. Chem.*, 2012, **402**, 1653-1666.